P- and S-wave velocity structure beneath SW British Columbia: constraints on serpentinized forearc mantle wedge

K. Ramachandran and R. D. Hyndman[1]

Pacific Geoscience Centre, Geological Survey of Canada, Sidney, B.C.,

Canada

K. Ramachandran, Pacific Geoscience Centre, Geological Survey of Canada, 9860 W Saanich Road, Sidney, B.C. V8L 4B2, Canada. (kramacha@nrcan.gc.ca)

R. D. Hyndman, Pacific Geoscience Centre, Geological Survey of Canada, 9860 W Saanich Road, Sidney, B.C. V8L 4B2, Canada. (hyndman@pgc.nrcan.gc.ca)

[1]Also: School of Earth and Ocean

Sciences, University of Victoria, Victoria,

British Columbia, Canada

This article describes 3-D high-resolution P-and S-wave velocity models (V_p, V_s) of the forearc crust and upper mantle beneath SW British Columbia, constructed from earthquake travel-time tomography. The forearc mantle wedge exhibits low velocities inferred to be due to hydration and serpentinization of the mantle peridotite by the fluids rising from the dehydrating Juan de Fuca slab. Low Poisson's ratio is inferred in the forearc crust just above the mantle wedge, possibly due to quartz deposited from rising silica-rich fluids. The Moho transition is inferred from a small increase in V_p and V_s at a depth of 36 km. The east dipping interface between the subducting oceanic crust and overlying forearc mantle is identified by higher values of V_p/V_s and Poisson's ratio in the forearc mantle, close to the interface. The serpentinization in the forearc mantle wedge decreases landward from 45 to 20% volume, using peridotite-antigorite V_p and V_s versus serpentinization relations. The total water content in a unit column of the forearc mantle increases landward from 500 m^3/m^2 near the mantle wedge corner to 2500 m^3/m^2 approaching the arc. About 25 m.y. of subduction is estimated to produce this amount of water from dehydration of the downgoing slab.

1. Introduction

This study presents tomographic seismic velocity results across the N. Cascadia forearc beneath SW British Columbia (Figure 1) where the Juan de Fuca oceanic plate converges with North America [e.g. *Riddihough and Hyndman*, 1991]. The depth to the Cascadia forearc Moho beneath southwestern British Columbia is ∼36 km [*Cassidy and Ellis*, 1993; *Ramachandran et al.*, 2005a]. Beneath the Strait of Georgia, *Zhao et al.* [2001] mapped low P-wave velocities at depths of 45–60 km and inferred forearc mantle serpentinization of 15–20%. *Bostock et al.* [2002] interpreted V_s perturbations across the continental Moho in northern Cascadia subduction zone as due to 50–60% serpentinized forearc mantle. *Ramachandran et al.* [2005a, 2005b] imaged the forearc upper mantle wedge beneath southeastern Vancouver Island and the Strait of Georgia from P-wave tomography and inferred ∼20% serpentinization of the forearc mantle. *Brocher et al.* [2003] summarized the evidence for low P- and S-wave velocities in the Cascadia forearc mantle wedge.

In this article, results from a P- and S-wave earthquake tomography study are presented in the form of vertical cross-sections of P- and S-wave velocity, V_p/V_s ratio and Poisson's ratio (σ). We emphasize the evidence for serpentinized forearc mantle in this region. The forearc Moho is inferred from the P- and S-wave velocity cross-sections to be at ∼36 km depth. The east dipping interface of the Juan de Fuca slab and the forearc mantle also is inferred from vertical-cross sections of V_p/V_s and σ. Volume percent serpentine in the forearc mantle, computed from the peridotite-antigorite V_p and V_s versus serpentinization relation, are then presented as vertical cross-sections.

2. Data and Methods

A three-dimensional travel-time tomographic inversion was used to construct P- and S-wave minimum structure velocity models from ∼70,000 P-wave travel-time picks and ∼28,000 S-wave travel-time picks from approximately 2,500 earthquakes. To maintain the consistency of P- and S-wave travel-time data, active-source P-wave travel-time data employed in the tomographic inversion by *Ramachandran et al.* [2005b] were not included. The velocity model was parameterized in the forward and inverse directions with a node and cell spacing of $(2 \times 2 \times 2)$ km and $(4 \times 4 \times 2)$ km, respectively. The P-wave velocity model and relocated hypocentral parameters were estimated using the regularized non-linear inversion method of *Zelt and Barton* [1998], modified to invert earthquake data [details in *Ramachandran et al.*, 2005a]. Earthquake locations from catalogue were used as the initial model for hypocentral parameters, and the initial 1-D velocity model of *Ramachandran et al.* [2005b] was used as the initial P-wave velocity model. Initial S-wave velocity model was constructed from the 1-D P-wave velocity model employing a V_p/V_s ratio of 1.75.

S-wave travel-time picks, and the relocated hypocentral positions obtained from the inversion of P-wave data were inverted for the S-wave velocity structure. The RMS travel-time misfit for the initial P- and S-wave travel-time data was 551 ms and 727 ms, respectively. The RMS travel-time misfit for the final P- and S-wave travel-time data was 207 ms and 282 ms, respectively. Rays were traced through the final models to compute the cells that received ray coverage. In order to maintain consistency of plots, the ray coverage obtained for the S-wave velocity model was employed to extract velocity for

cells with ray coverage for both P- and S-wave velocity data, since there is relatively less S-wave data.

3. Results

P- and S-wave velocity cross-section along profile AB (Figure 1) is shown in Figure 2a and 2b respectively. V_p/V_s and σ computed from P- and S-wave velocity along profile AB is shown in Figure 2c and 2d. The inferred positions of the Juan de Fuca slab and the forearc mantle are shown on the cross-sections. The location of the slab mapped in the present study from S-wave velocity is consistent with the position of the slab inferred in previous tomographic P-wave velocity models by *Ramachandran et al.* [2005a, 2005b]. The P- and S-wave velocity models from the present study distinctly image the position of the forearc mantle. The forearc mantle wedge is imaged with low P-wave velocities of 7.4–7.8 km/s, and S-wave velocities of 4.1–4.4 km/s.

4. Discussion

4.1. Forearc Crust

Poisson's ratio of most of the forearc crust is in the range of 0.24–0.27, which is within the range of 0.25±0.04 quoted for Mesozoic/Cenozoic orogenic belts [*Zandt and Ammon*, 1995]. A relative high velocity zone ($V_p > 6.8$ km/s, $V_s > 3.8$ km/s, and $\sigma \sim .25$) is imaged in the mid crust between 70–100 km model distance, and at 15–25 km depth (Figures 2a, 2b, and 2d). These values are similar to the values for greenschist facies rocks ($V_p > 6.9$ km/s, $V_s > 3.9$ km/s, and $\sigma \sim .26$) [*Christensen*, 1996] such as meta-gabbro that are possibly associated with the basal part of the Eocene Volcanic Crescent Terrane. Poisson's ratio of the lower crust above the forearc mantle wedge is in the range

of 0.20–0.24. Poisson's ratio of quartz is 0.09 [*Christensen*, 1996], and quartz deposited in the lower forearc crust, above the mantle wedge, from rising silica-rich fluids [e.g *Breeding and Ague*, 2002] is a possible explanation for the low σ values in this region.

4.2. Forearc Moho

In the Cascadia subduction zone to the west of the volcanic front, there is no reflection signature of the forearc Moho in deep seismic sections suggesting a small impedance contrast or gradient boundary [e.g. *Brocher et al.* 2003]. In our P-wave velocity model (Figure 2a), between 150 and 180 km, there is a rapid velocity increase from 6.8 to 7.4 km/s between 35 and 40 km depth, inferred to be the crust-mantle transition (forearc Moho). There also is a velocity increase observed in the S-wave velocity model (Figure 2b). Reduction of velocities by hydration and serpentinization of the forearc mantle is the probable reason for the absence of the normal Moho with a P-wave velocity contrast of 1.2–1.4 km/s. However, the forearc Moho is distinguishable as a rapid increase in P- and S-wave velocities between 35 and 40 km depth (Figures 2a and 2b). These results are consistent with the ∼36 km Moho depth in the Strait of Georgia (∼120 km to the north) from receiver function studies [*Cassidy and Ellis*, 1993], but we do not see the shear impedance inversion (high velocity crust over lower velocity mantle) inferred by *Bostock et al.* [2002]. In the vertical-cross sections of V_p/V_s and σ, the east dipping interface of the Juan de Fuca crust and the forearc mantle is clearly identified by the contrasting values across the interface.

4.3. Forearc Mantle Serpentinization

Many authors have concluded that large amounts of fluids are carried into the mantle by subducting slabs [e.g. *Peacock*, 1990]. The estimated fluid expulsion rate from the subducting Juan de Fuca slab, beneath the Cascadia forearc mantle, is $\sim 0.0001\, m^3/m^2 yr$ [e.g. *Hyndman and Peacock*, 2003]. The expelled fluids are inferred to rise, hydrate, and serpentinize the forearc mantle peridotite. However we recognize that low velocities in the mantle wedge can also be attributed to 1) presence of chlorite with antigorite, 2) anisotropy of the serpentinized peridotite, and 3) high pore pressure [*Christensen*, 2004]. Of the main serpentine minerals, chrysotile and lizardite have similar composition and elastic properties and are stable below 300°C. Antigorite is the stable species of serpentine at forearc mantle P-T conditions. *Bostock et al.* [2002] interpreted V_s perturbations across continental Moho in northern Cascadia subduction zone as due to serpentinized mantle and discussed the presence of antigorite serpentine, but computed serpentine contents from the available data on the elastic properties of chrysotile-lizardite assemblages which, as emphasized by *Christensen* [2004], have a larger effect on velocity.

The tomographic velocity imaged in the uppermost northern Cascadia forearc mantle is anomalously low compared to the normal Pn velocity of 8.15–8.25 km/s in stable continental areas for an estimated Moho temperature of 350–450°C [e.g., *Hyndman and Peacock*, 2003]. In three-dimensional seismic tomography, velocity is estimated by employing ray paths oriented in many possible directions. Hence, if there is anisotropy, tomographic velocities are approximately the mean of the P- and S-wave velocities in x, y and z directions. The Cascadia forearc is relatively cool as a consequence of heat removed by

the subduction of cool near surface oceanic crust. Observed heat flow in this region is in agreement with the subduction thermal model and calculated forearc mantle temperature is in the range of 400–600°C [*Hyndman and Wang*, 1995]. V_p of peridotite taken to be the average *Pn* velocity for cool stable areas of 8.2 km/s [*Christensen and Mooney*, 1995] is utilized in our study. Employing a V_p/V_s value of 1.75, the unaltered upper mantle V_s is taken as 4.7 km/s. V_p and V_s values of antigorite at 1 GPA and 500°C are taken from *Christensen* [2004]. The plot of peridotite-antigorite velocity versus volume percent serpentinization is shown in Figure 3.

V_p (7.4–7.8 km/s) and V_s(4.1–4.4 km/s) of the forearc mantle from our study indicate 20–45% serpentinization in the mantle wedge (Figure 3). Complete alteration of peridotite to pure serpentine increases the bound water content by ∼13 wt%, and the variation of water content with velocity is nearly linear [e.g. *Carlson and Miller*, 2002], so our study indicates water contents in the forearc mantle of 2–6 wt%. σ of peridotite is 0.25 (V_p/V_s=1.75), and antigorite 0.29 (V_p/V_s=1.84), so our forearc mantle σ of ∼0.27 (V_p/V_s ∼1.8) is consistent with the above estimates of volume percent serpentinization. Lack of detailed knowledge on the other processes that may be responsible for lowering of forearc mantle velocities precludes the possibility of estimating their contribution to lowering velocities. Hence, the forearc mantle serpentinization values of 20–40% are a maximum.

The percent serpentinization in the forearc mantle-wedge computed from *P*- and *S*-wave velocities (Figures 4a and 4b) show higher levels of serpentinization near the slab-forearc mantle corner, ∼40%, decreasing landward to about ∼20% approaching the volcanic arc

(Figure 4c). At 500° C and 1 GPA, the density of water is $\sim$ 1010 kg/m^3 [e.g. *Verma*, 2003], and the total water content computed for a unit column of the forearc mantle ranges from 500 m^3/m^2 near the mantle wedge corner to 2500 m^3/m^2 approaching the arc (Figure 4c). At a rate of production from the slab of about 0.0001 m^3/m^2 yr [e.g. *Hyndman and Peacock*, 2003] the later amount would be produced in $\sim$25 m.y. of subduction.

Acknowledgments. Geological Survey of Canada Contribution.

References

Bostock, M. G., R. D. Hyndman, S. Rondenay, and S. M. Peacock (2002), An inverted continental Moho and the serpentinization of the forearc mantle, *Nature*, *417*, 536–538.

Breeding, C. M., and J. J. Ague (2002), Slab-derived fluids and quartz-vein formation in an accretionary prism, Otago Schist, New Zealand, *Geology*, *30*, 499–502.

Brocher, T. M., T. Parsons, A. M. Tréhu, C. M. Snelson, and M. A. Fisher (2003), Seismic evidence for widespread serpentinized forearc upper mantle along the Cascadia margin, *Geology*, *31*, 267–270.

Carlson, R. L., and D. J. Miller (2003), Mantle wedge water contents estimated from seismic velocities in partially serpentinized peridotites, *Geophys. Res. Lett.*, *30*, 1250, doi:10.1029/2002GL016600.

Cassidy, J. F. and R. M. Ellis (1993), S-wave velocity structure of the northern Cascadia subduction zone, *J. Geophys. Res. 98*, 4407–4421.

Christensen, N. I. (1996), Poisson's ratio and crustal seismology, *J. Geophys. Res. 101*, 3139–3156.

Christensen, N. I. (1966), Elasticity of ultrabasic rocks, *J. Geophys. Res. 71*, 5921–5931.

Christensen, N. I. (2004), Serpentines, Peridotites, and Seismology, *International Geology Review*, *46*, 795–816.

Christensen, N. I. and W. D. Mooney (1995), Seismic velocity structure and composition of the continental crust: A global view, *J. Geophys. Res.*, *100*, 9761–9788.

Hyndman, R. D. and S. M. Peacock (2003), Serpentinization of the forearc mantle, *Earth and Planetary Science Letters*, *212*, 417–432.

Hyndman, R. D., and K. Wang (1995), The rupture zone of Cascadia great earthquakes from current deformation and the thermal regime, *J. Geophys. Res.*, *100*, 22133–22154, doi:10.1029/95JB01970.

Peacock, S.M. (1990), Fluid processes in subduction zones, *Science*, *248*, 329–337.

Ramachandran, K., S. E. Dosso, G. D. Spence, R. D. Hyndman, and T. M. Brocher (2005a), Forearc structure beneath southwestern British Columbia: A three-dimensional tomographic velocity model, *J. Geophys. Res.*, *110*, B02303, doi:10.1029/2004JB003258.

Ramachandran, K., R. D. Hyndman, and T. M. Brocher (2005b), Northern Cascadia Subduction Zone: Tomographic 3D *P*-wave Velocity Structure, *Geophys. J. Int.*, (in review).

Riddihough, R. P. and R. D. Hyndman (1991), Modern plate tectonic regime of the continental margin of western Canada, *In* Geology of the Cordilleran Orogen in Canada, *Edited by* H. Gabrielse and C.J. Yorath, Geology of Canada, *4*, 435–455, Geological Survey of Canada.

Verma, M.P. (2003), Steam tables for pure water as an ActiveX component in Visual Basic 6.0, *Computers and Geosciences*, *29*, 1155–1163.

Zandt, G. and C. J. Ammon (1995), Continental crust composition constrained by measurements of crustal Poisson's ratio, *Nature*, *374*, 152–154.

Zhao, D., K. Wang, G. C. Rogers, and S. M. Peacock (2001), Tomographic image of low P velocity anomalies above slab in northern Cascadia subduction zone: *Earth, Planets, and Space*, *53*, 285–293.

Zelt, C. A. and P. J. Barton (1998), 3–D Seismic refraction tomography: A comparison of two methods applied to data from the Faroe basin, *J. Geophys. Res.*, *103*, 7187–7210.

Figure Captions

Figure 1. Location map of the study region. Vertical cross-sections of P- and S-wave velocity along profile AB is shown in Figure 2.

Figure 2. Vertical cross-section along profile AB showing a) P-wave velocity, b) S-wave velocity, c) V_p/V_s ratio and d) Poisson's ratio (σ). The red box in Figure 2d shows the region for which volume percent serpentinization is shown in Figure 4.

Figure 3. Plot of peridotite-antigorite assemblage velocity versus volume percent serpentinization.

Figure 4. Plot of volume percent serpentinization in the forearc mantle computed from a) P-wave velocity and b) S-wave velocity for the region enclosed by the red box in Figure 2d, c) Plot of average volume% serpentine and total water content in a unit column of the forearc mantle.

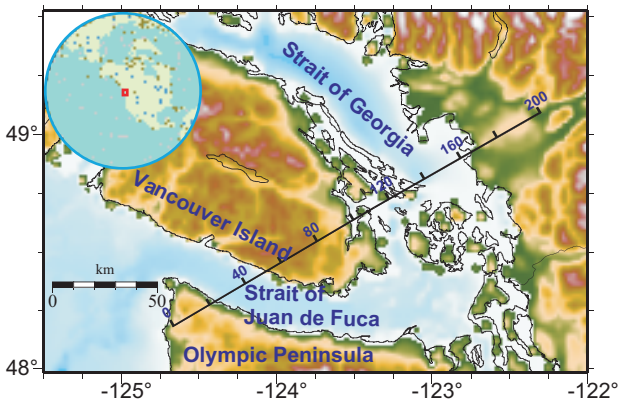
Strait of Georgia
Vancouver Island
Strait of
Juan de Fuca
Olympic Peninsula
km
0
50
0
40
80
120
160
200
49°
48°
-125°
-124°
-123°
-122°

Figure 1

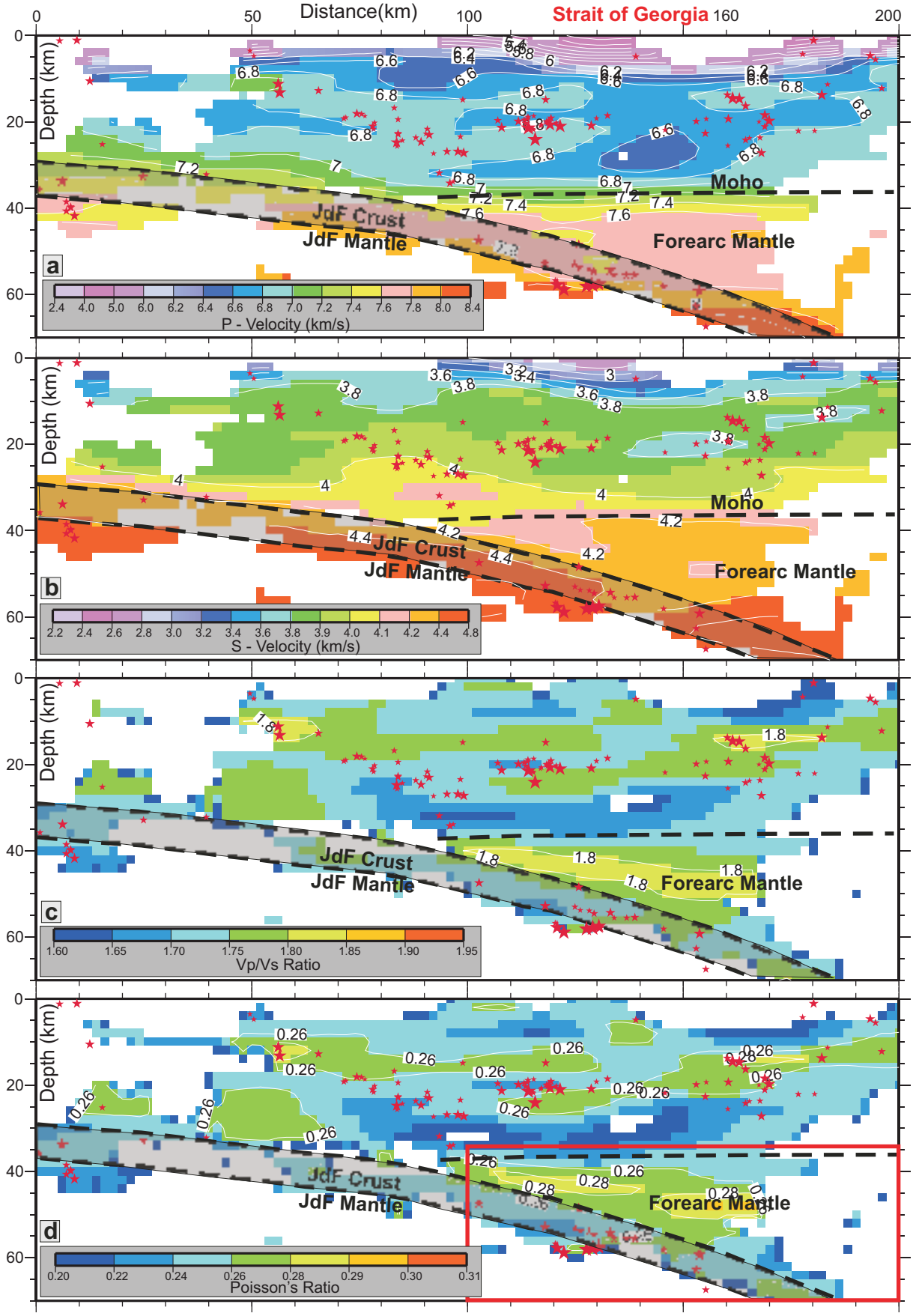
Distance(km)
Strait of Georgia
Depth (km)
Moho
JdF Crust
JdF Mantle
Forearc Mantle
a
P - Velocity (km/s)
b
S - Velocity (km/s)
c
Vp/Vs Ratio
d
Poisson's Ratio

Figure 2

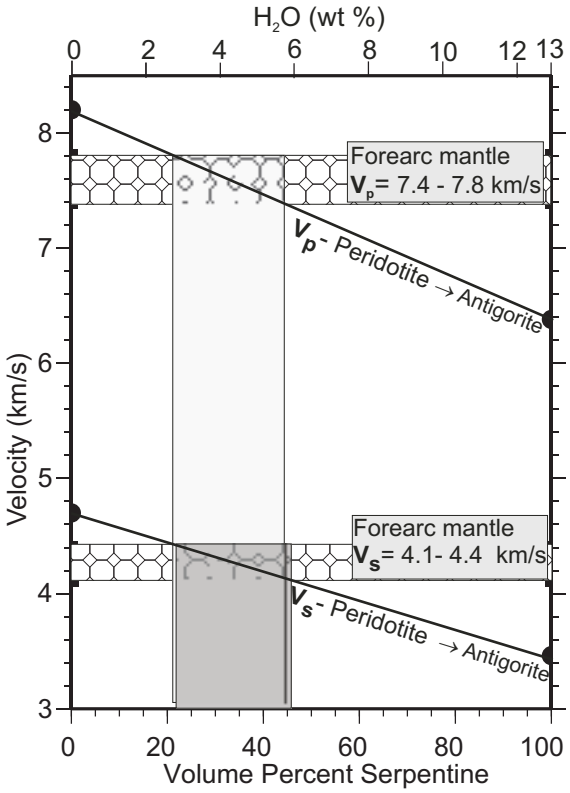
H2O (wt %)
0
2
4
6
8
10
12
13
Forearc mantle
Vp= 7.4 - 7.8 km/s
Vp - Peridotite → Antigorite
Forearc mantle
Vs= 4.1- 4.4 km/s
Vs - Peridotite → Antigorite
Velocity (km/s)
8
7
6
5
4
3
0
20
40
60
80
100
Volume Percent Serpentine

Figure 3

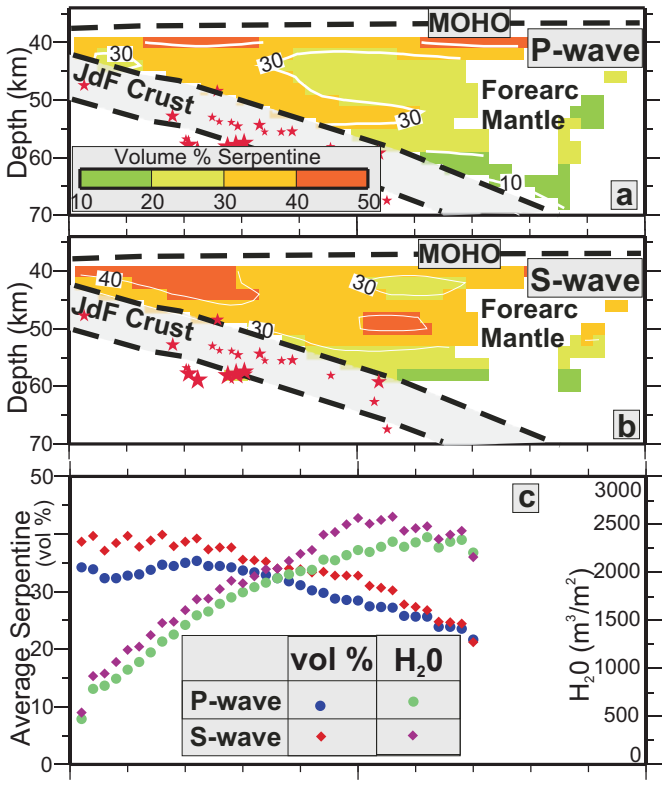
MOHO
P-wave
JdF Crust
Forearc
Mantle
Volume % Serpentine
10 20 30 40 50
Depth (km)
a
MOHO
S-wave
JdF Crust
Forearc
Mantle
b
c
Average Serpentine (vol %)
H2O (m3/m2)
vol %
H2O
P-wave
S-wave

Figure 4